

# Effect of Cu as Minority Alloying Element on Glass Forming Ability and Crystallization Behavior of Rapidly Solidified Al-Si-Ni Ribbons

Vanya Dyakova  
IMSETHAC-BAS

Materials Testing and Analyses  
Sofia, Bulgaria  
v\_diakova@ims.bas.bg

Hristina Spasova  
IMSETHAC-BAS

Materials Testing and Analyses  
Sofia, Bulgaria  
h.spasova@ims.bas.bg

Yoanna Kostova  
IMSETHAC-BAS

Materials Testing and Analyses  
Sofia, Bulgaria  
y\_kostova@ims.bas.bg

Yana Mourdjeva  
IMSETHAC-BAS

Materials Testing and Analyses  
Sofia, Bulgaria  
yana@ims.bas.bg

Georgi Stefanov  
IMSETHAC-BAS

Metal science  
Sofia, Bulgaria  
stefanov.g@gmail.com

**Abstract.** The influence of copper as a minority alloying element in the process of rapid solidification of Al-Si-Ni ribbons produced by Chill Block Melt Spinning (CBMS) was investigated. XRD and TEM analyses proved a completely amorphous structure of the alloys  $Al_{74}Ni_{16}Si_{10}$  and  $(Al_{74}Ni_{16}Si_{10})_{98}Cu_2$ . The crystallization behaviour of these alloys was studied by DSC analysis. It was found that the crystallization of the amorphous alloys  $(Al_{74}Ni_{16}Si_{10})_{100-x}Cu_x$ ,  $x=0, 2$  runs in two steps. The temperatures  $T_{x1}$  and  $T_{x2}$  of each of the crystallization steps were determined. It was proven that the addition of 2 at. % copper does not significantly change  $T_x$  temperatures. The temperature difference  $\Delta T_x$  was calculated and it showed that more thermally stable is the copper containing alloy. Crystalline analogues of the amorphous alloys were obtained by annealing of the melt-spun amorphous ribbons at a temperature which exceeded by 170°C the onset crystallization temperature. The type and size of separated crystalline phases were determined by XRD. It was found that the addition of 2 at. % Cu to  $Al_{74}Ni_{16}Si_{10}$  alloy causes a separation of new phases -  $Cu_{3.8}Ni$  and  $(Al, Cu)Ni_3$  and 54%, 24% and 7% size increase of the phases Al,  $Al_3Ni$ ,  $NiSi_2$  respectively.

**Keywords:** amorphous, nanocrystalline, aluminum, copper, silicon, nickel.

## I. INTRODUCTION

The first amorphous alloys were obtained as ribbons about sixty years ago, but the interest in them continues to be great, due to their good mechanical and physical properties and their high corrosion resistance. The most promising applications of amorphous alloys are considered to be in the field of electronics and electrical engineering. Initially, mainly iron-based amorphous alloys were studied, but in recent decades the interest in aluminum-based amorphous alloys is constantly growing [1] – [4]. Over the past decade, scientists' research has focused on studying the properties of both amorphous composites [5] and amorphous foams [6].

Amorphous aluminum alloys are generally produced from various Al-TM-RE ternary alloy compositions (TM are transition metals, RE are rare earth elements). The resulting alloys show great glass-forming ability (GFA) and high mechanical strength [7] – [11], but they contain expensive rare earth elements, which we tried to replace with cheaper ones. In our previous studies, we obtained rapidly solidified ribbons of the Al-Cu-Mg system alloyed with minority amounts of Zn, Zr and Ni and studied the influence of these elements on the GFA, crystallization and corrosion behavior on the newly produced alloys [12] – [14].

Print ISSN 1691-5402

Online ISSN 2256-070X

<https://doi.org/10.17770/etr2023vol3.7200>

© 2023 Vanya Dyakova, Hristina Spasova, Yoanna Kostova, Yana Mourdjeva, Georgi Stefanov.

Published by Rezekne Academy of Technologies.

This is an open access article under the [Creative Commons Attribution 4.0 International License](https://creativecommons.org/licenses/by/4.0/).

The aim of this research is to obtain amorphous alloys from the Al-Si-Ni system and study the influence of Cu as a minority alloying element on the GFA and crystallization behavior on the Al-Si-Ni-Cu rapidly solidified amorphous ribbons.

## II. MATERIALS AND METHODS

The base Al-Si-Ni and Al-Si-Ni-Cu alloy were synthesized from pure metals Al 99.99 %, Ni 99.99, Cu 99.99 and pure Si 99.99% in a plant comprising a resistance electric furnace installed in a water-cooled pneumo-vacuum chamber in argon atmosphere of 99.998 % purity.

The Chill Block Melt Spinning (CBMS) method was used to obtain rapidly solidified ribbons about 3 - 4 mm wide and 26 - 40  $\mu\text{m}$  thick. The production processes of the ligatures and the rapidly solidified ribbons are described in details in our previous publications [12] – [14].

Samples of the base Al-Si-Ni and of the Al-Si-Ni-Cu rapidly solidified ribbons were annealed for 2 hours at 350°C in argon atmosphere for the purposes of devitrification. The chemical composition of the produced rapidly solidified ribbons was determined by Energy Dispersive X-ray Spectroscopy (EDS) analysis using a scanning electron microscope HIROX 5500 with EDS system BRUCKER at a magnification of 100x in 10 fields with a field area of 2.5  $\text{mm}^2$ .

X-ray diffraction (XRD) analysis was performed to characterize the amount of amorphous and crystalline phases and to determine the phase composition of the crystalline part of the ribbons before and after devitrification. A Bruker D8 Advance powder X-ray diffractometer with Cu  $K\alpha$  radiation (Ni filter) and LynxEye recording in a solid-state position-sensitive detector was applied. The PDF-2 (2009) database of the International Data Diffraction Center (ICDD) and the DiffracPlusEVA software package were used to perform the qualitative phase analysis.

The microstructure of Al-Si-Ni and Al-Si-Ni-Cu rapidly solidified ribbons was studied by transmission electron microscope (TEM) JEOL 1011 at accelerating voltage of 100 kV.

Differential scanning calorimetry (DSC) analysis was performed on STA 449 F3 Jupiter calorimeter connected to a QMS 403 Aëolos Quadro mass spectrometer in Ar environment. The rate of the protective Ar flow in the apparatus during the analysis was 30  $\text{mL s}^{-1}$  and the flow rate of the purge Ar through the studied samples was 20  $\text{mL s}^{-1}$ . The heating rate was 20  $\text{K min}^{-1}$ .

## III. RESULTS AND DISCUSSIONS

The results of EDS analyses of the chemical composition of rapidly solidified ribbons Al-Si-Ni and Al-Si-Ni-Cu are presented in Table 1. Based on the obtained EDS results the Al-Ni-Si alloy will be denoted further as  $\text{Al}_{74}\text{Ni}_{16}\text{Si}_{10}$ . EDS analysis showed that the Cu content in the Al-Si-Ni-Cu rapidly solidified ribbon was close to 2 at.

% Cu, therefore, in our work, it will be denoted respectively  $(\text{Al}_{74}\text{Ni}_{16}\text{Si}_{10})_{98}\text{Cu}_2$ .

TABLE 1 CHEMICAL COMPOSITION OF THE RAPIDLY SOLIDIFIED RIBBONS AL-NI-SI AND AL-NI-SI-CU

Designation of ribbons	Al [at. %]	Ni [at. %]	Si [at. %]	Cu [at. %]
$\text{Al}_{74}\text{Ni}_{16}\text{Si}_{10}$	73.50	16.08	10.42	-
$(\text{Al}_{74}\text{Ni}_{16}\text{Si}_{10})_{98}\text{Cu}_2$	73.97	14.94	8.76	2.33

The XRD patterns of  $\text{Al}_{74}\text{Ni}_{16}\text{Si}_{10}$  and  $(\text{Al}_{74}\text{Ni}_{16}\text{Si}_{10})_{98}\text{Cu}_2$  ribbons before and after annealing and XRD-results on their structural characteristics are presented in Fig. 1 and in Table 2.

A well-defined halo is present in the XRD patterns of each of the two studied rapidly solidified ribbons (Fig. 1 (a), Fig. 1 (b)), which is an evidence of their amorphous structure. Further, in our work, these alloys will be denoted by the index "am".

The results of XRD analyzes of the amorphous structure of the rapidly solidified  $\text{Al}_{74}\text{Ni}_{16}\text{Si}_{10}$  and  $(\text{Al}_{74}\text{Ni}_{16}\text{Si}_{10})_{98}\text{Cu}_2$  ribbons were confirmed by TEM observations and electron diffraction. The diffractograms of the two alloys showed a well-defined diffraction halo and no diffraction spots, which proved that their structure was completely amorphous.

The TEM image of the microstructure of  $\text{Al}_{74}\text{Ni}_{16}\text{Si}_{10}$  alloy (Fig. 2 (a)) showed the typical for metallic glass uniform matrix. Small white spots were observed in the dark matrix of  $(\text{Al}_{74}\text{Ni}_{16}\text{Si}_{10})_{98}\text{Cu}_2$ . The absence of phase boundaries and of diffraction pixels makes us to consider they are clusters of atoms of smaller atom number (probably Al) which have formed during rapid solidification but have not succeeded to combine into a crystal lattice. The bright contrast in TEM image is due to the lower electron absorption resulting on the smaller atom number of aluminium (Fig. 2 (b))

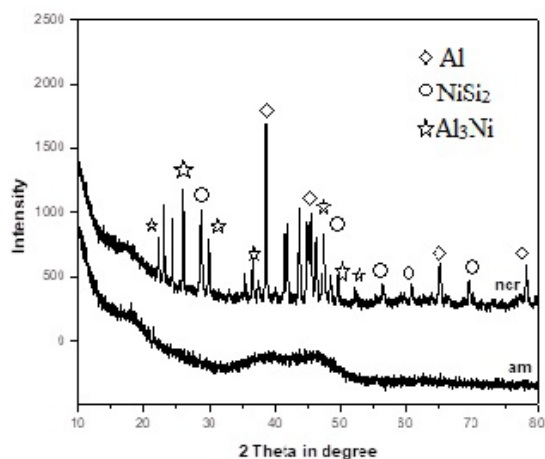
XRD analysis of the amorphous alloys subject to annealing at 350°C showed complete crystallization. Peaks of three types of crystalline phases were found in  $\text{Al}_{74}\text{Ni}_{16}\text{Si}_{10}$  alloy: Al,  $\text{Al}_3\text{Ni}$  and  $\text{NiSi}_2$  (Fig. 1 (a)) and five types of crystalline phases in  $(\text{Al}_{74}\text{Ni}_{16}\text{Si}_{10})_{98}\text{Cu}_2$

alloy: Al,  $\text{Al}_3\text{Ni}$ ,  $\text{NiSi}_2$ ,  $\text{Cu}_{3,8}\text{Ni}$  and traces of (Al, Cu) $\text{Ni}_3$  (Fig. 1 (b)).

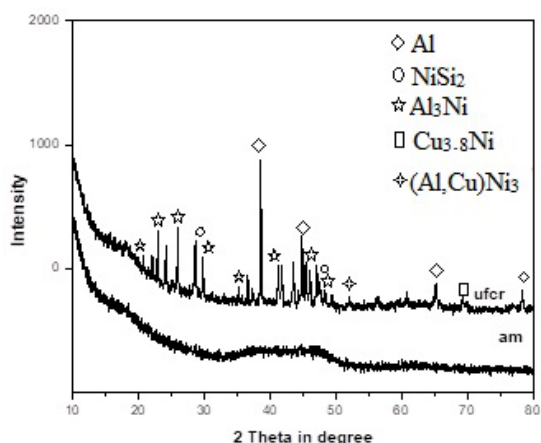
The quantity and the size of the crystalline phases were determined as nanosized in  $\text{Al}_{74}\text{Ni}_{16}\text{Si}_{10}$  and as ultrafine in  $(\text{Al}_{74}\text{Ni}_{16}\text{Si}_{10})_{98}\text{Cu}_2$  (Table 2). This gives us the reason to designate the annealed  $\text{Al}_{74}\text{Ni}_{16}\text{Si}_{10}$  alloy as nanocrystalline and the annealed  $(\text{Al}_{74}\text{Ni}_{16}\text{Si}_{10})_{98}\text{Cu}_2$  alloy as ultrafine and to use for them the indexes "ncr" and "ufcr", respectively [15].

TABLE 2 STRUCTURAL CHARACTERISTICS OF AMORPHOUS AND CRYSTALLINE  $Al_{74}Ni_{16}Si_{10}$  AND  $(Al_{74}Ni_{16}Si_{10})_{98}Cu_2$  ALLOYS

Designation of the alloy	Components of the crystal part		
	Types of phases	Quantity of the phase [mass. %]	Phase size [nm]
$Al_{74}Ni_{16}Si_{10}$ am	-	-	-
$Al_{74}Ni_{16}Si_{10}$ ncr	Al -fcc	16	88
	$Al_3Ni$ Orthorombic	72	71
	$NiSi_2$ -fcc	12	43
$(Al_{74}Ni_{16}Si_{10})_{98}Cu_2$ am	-	-	-
$(Al_{74}Ni_{16}Si_{10})_{98}Cu_2$ ufer	Al -fcc	19	136
	$Al_3Ni$ Orthorombic	64	88
	$NiSi_2$	13	45
	$Cu_{3.8}Ni$ - fcc	4	60
	$(Al,Cu)Ni_3$ -fcc	traces	



(a)  $Al_{74}Ni_{16}Si_{10}$ .



(b)  $(Al_{74}Ni_{16}Si_{10})_{98}Cu_2$

Fig. 1. XRD diagrams of  $Al_{74}Ni_{16}Si_{10}$  and  $(Al_{74}Ni_{16}Si_{10})_{98}Cu_2$  alloys.

XRD results showed that the addition of only 2 at. % Cu to  $Al_{74}Ni_{16}Si_{10}$  alloy caused a 54%, 24% and 7% size increase of the nanocrystalline phases Al,  $Al_3Ni$ ,  $NiSi_2$

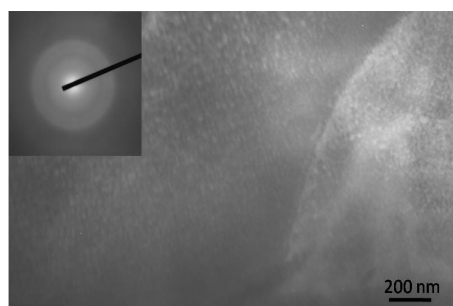
respectively, and a separation of two new phases –  $Cu_{3.8}Ni$  and  $(Al, Cu)Ni_3$ . The increased sizes, especially of the Al-containing phases can be well seen when comparing the TEM images of the two alloys (Fig. 2 (c) and 2 (d)).

Fig. 3 and Fig. 4 show DSC diagrams of  $Al_{74}Ni_{16}Si_{10}$  and  $(Al_{74}Ni_{16}Si_{10})_{98}Cu_2$  alloys in amorphous (a)-solid line and in crystalline (b) - dotted line state. The results of the DSC analyses are presented in Table 3. The DSC diagrams of each of the amorphous alloys have two exothermic peaks, indicating that crystallization takes place in two separate steps. There is no clear evidence of the glass transition effect before the temperatures of the first exothermic crystallization peak of both alloys. The absence of a glass transition (GT) feature can be explained by the formation of significant number of clusters during rapid solidification, evidence of which we observed in Fig. 2 (b). With continued heating, clusters of size above the critical nucleation size grow even at lower temperatures. Therefore, we assume that  $T_g = T_{x1}$  peak and that the GT effect is hidden below the first crystallization peak. The same vitrification effect has been observed in amorphous aluminum-based alloys by other researchers [16], [17].

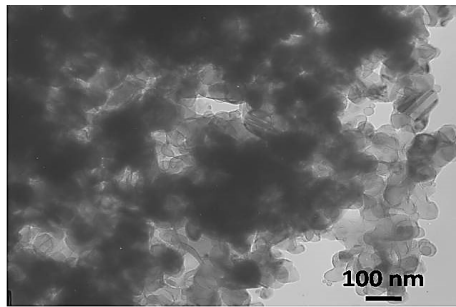
They assumed that the difference  $\Delta T_x$  between the crystallization temperature and the glass transition temperature, which mostly determines the so called supercooled liquid region of the amorphous alloy, in this case can be calculated as  $\Delta T_x = T_{x2} - T_{x1}$  [17]. The parameter  $\Delta T_x$  is directly associated with the glass stability (GS) of the alloy and it is an indication of the resistance to devitrification by the annealing above  $T_g$ . For our amorphous alloys the values of  $\Delta T_x$  are 64K and 92K for the  $Al_{74}Ni_{16}Si_{10}$  and  $(Al_{74}Ni_{16}Si_{10})_{98}Cu_2$  alloys respectively. This clearly indicates that the partial replacement of Si and Ni atoms by Cu improves the ability of the melt to form glasses [17].



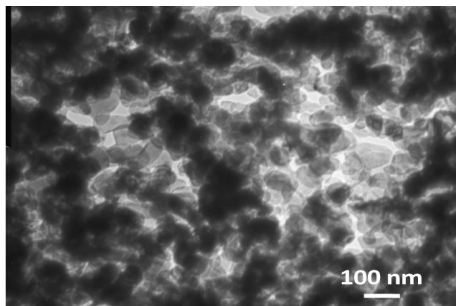
(a)  $Al_{74}Ni_{16}Si_{10}$  - am



(b)  $(Al_{74}Ni_{16}Si_{10})_{98}Cu_2$ - am



(c) Al<sub>74</sub>Ni<sub>16</sub>Si<sub>10</sub>- ncr



(d) (Al<sub>74</sub>Ni<sub>16</sub>Si<sub>10</sub>)<sub>98</sub>Cu<sub>2</sub> - ufer

Fig. 2. Microstructure of the amorphous (a), (b) and crystalline (c), (d) Al<sub>74</sub>Ni<sub>16</sub>Si<sub>10</sub> and (Al<sub>74</sub>Ni<sub>16</sub>Si<sub>10</sub>)<sub>98</sub>Cu<sub>2</sub> alloys, TEM.

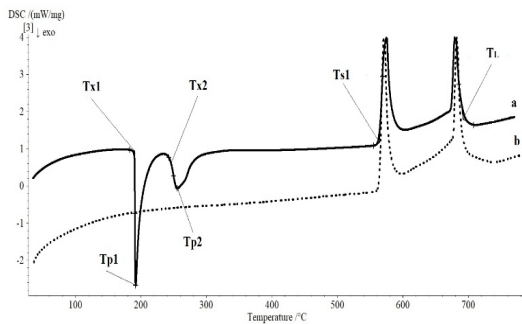


Fig. 3. DSC diagrams of Al<sub>74</sub>Ni<sub>16</sub>Si<sub>10</sub> alloy (a) amorphous; (b) nanocrystalline.

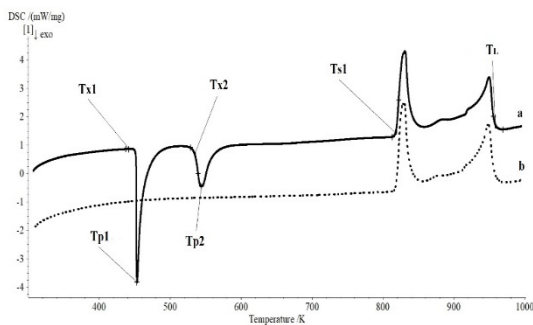


Fig. 4. DSC diagrams of (Al<sub>74</sub>Ni<sub>16</sub>Si<sub>10</sub>)<sub>98</sub>Cu<sub>2</sub> alloy (a) amorphous; (b) ultrafinecrystalline.

TABLE 3 RESULTS OF DSC ANALYSIS OF AMORPHOUS Al<sub>74</sub>Ni<sub>16</sub>Si<sub>10</sub> AND (Al<sub>74</sub>Ni<sub>16</sub>Si<sub>10</sub>)<sub>98</sub>Cu<sub>2</sub> ALLOYS

	Al <sub>74</sub> Ni <sub>16</sub> Si <sub>10</sub> - am	(Al <sub>74</sub> Ni <sub>16</sub> Si <sub>10</sub> ) <sub>98</sub> Cu <sub>2</sub> - am
Tx1, [K]	453	452
Tpeak, [K]	465	453
Tx2, [K]	529	535
Tpeak2, [K]	529	544
Ts, [K]	838	819
Tl, [K]	965	954
ΔTx, [K]	64	92

#### IV. CONCLUSIONS

Rapidly solidified amorphous ribbons Al<sub>74</sub>Ni<sub>16</sub>Si<sub>10</sub> and (Al<sub>74</sub>Ni<sub>16</sub>Si<sub>10</sub>)<sub>98</sub>Cu<sub>2</sub> and their crystalline analogues were produced by the Chill Block Melt Spinning (CBMS) method and by subsequent annealing of the amorphous alloys for 2 hours at 350°C.

It was found by DSC analyses that the crystallization of the amorphous alloys Al<sub>74</sub>Ni<sub>16</sub>Si<sub>10</sub> and (Al<sub>74</sub>Ni<sub>16</sub>Si<sub>10</sub>)<sub>98</sub>Cu<sub>2</sub> takes place in two steps. It was proven that the addition of 2 at. % copper to the Al<sub>74</sub>Ni<sub>16</sub>Si<sub>10</sub> alloy does not significantly change the T<sub>g</sub> temperature, but improve the glass forming ability of (Al<sub>74</sub>Ni<sub>16</sub>Si<sub>10</sub>)<sub>98</sub>Cu<sub>2</sub> alloy.

It was found that the addition of 2 at. % Cu to nanocrystalline Al<sub>74</sub>Ni<sub>16</sub>Si<sub>10</sub> alloy causes a 54%, 24% and 7% size increase of the separated crystalline phases Al, Al<sub>3</sub>Ni, NiSi<sub>2</sub> respectively, and a separation of new Cu<sub>3,8</sub>Ni and (Al, Cu)Ni<sub>3</sub> phases in the ultrafine crystalline (Al<sub>74</sub>Ni<sub>16</sub>Si<sub>10</sub>)<sub>98</sub>Cu<sub>2</sub> alloy.

#### V. ACKNOWLEDGEMENTS

This study is funded by the project “Study of the rheological and corrosion behavior of amorphous and nanocrystalline aluminum-based alloys”, Contract with BNSF №KP-06-H37/13 of 06 December 2019.

A part of experimental units used in this work was funded by the European Regional Development Fund within the OP “Science and Education for Smart Growth 2014 - 2020”, project CoE “National center of mechatronics and clean technologies”, No BG05M2OP001-1.001-0008-C08.

The authors are indebted to our colleagues prof. Stoyko Gyurov, PhD, Jordan Georgiev, PhD, Ivan Penkov, PhD (IMSETHAC-BAS) and prof. Daniela Kovacheva, PhD, ass. prof. Nikolay Marinkov, PhD (IIC – BAS) for their

help and support in the preparation and for the XRD and DSC analyzes of the alloys.

#### REFERENCES

- [1] Y. H. Kim., K. Hiraga, A. Inoue, T. Masumoto , H. H. Jo, “Crystallization and High Mechanical Strength of Al-Based Amorphous Alloys” *Materials Transactions, JIM*, vol. 35, pp. 293-302, 1994, <https://doi.org/10.2320/matertrans1989.35.293>
- [2] H. Kim, A. Inoue and T. Masumoto, “High Strength Bulk Amorphous Alloys with Low Critical Cooling Rates (Overview)”, *Material Transactions, JIM*, vol. 36, , no. 7, pp.866-875,1995 <https://doi.org/10.2320/matertrans1989.36.866>
- [3] I. T. H Chang, R. R. Botten, “Heat treatment of rapidly solidified Al-Ni-Mn alloys”, *Materials Science and Engineering: A*, vol. 226-228, pp.183-186, 1997 [https://doi.org/10.1016/S0921-5093\(97\)80035-4](https://doi.org/10.1016/S0921-5093(97)80035-4)
- [4] W. Kim, M. Gogebakan, B. Cantor, “Heat treatment of amorphous Al85Y5Ni10 and Al85Y10Ni5 alloys”, *Materials Science and Engineering: A*, vol. 226–228, , pp.178-182, 1997 [https://doi.org/10.1016/S0921-5093\(96\)10613-4](https://doi.org/10.1016/S0921-5093(96)10613-4)
- [5] I. Permyakova, A. Glezer, “Amorphous-Nanocrystalline Composites Prepared by High-Pressure Torsion”, *Metals*, vol.10, no. 4, p.511, 2020 <https://doi.org/10.3390/met10040511>
- [6] A. H. Brothers, D. C. Dunand, “Amorphous metal foams”, *Scripta Materialia*, vol. 54, no. 4, , pp. 513-520, 2006 <https://doi.org/10.1016/j.scriptamat.2005.10.048>
- [7] M. Gögebakan, O. Uzun, T. Karaaslan, M. Keskin, “Rapidly solidified Al–6.5 wt. % Ni alloy”, *Journal of Materials Processing Technology*, vol. 142, no.1, pp. 87-92, 2003, <https://www.sciencedirect.com/science/article/abs/pii/S0924013603004667>
- [8] M. A. Munoz-Morris, S. Surinach, M. Gich, M. D. Baro, D. G. Morris, “Crystallization of a Al–4Ni–6Ce glass and its influence on mechanical properties”, *Acta Materialia*, 51, , pp. 1067-1077, 2003 [https://doi.org/10.1016/S1359-6454\(02\)00511-6](https://doi.org/10.1016/S1359-6454(02)00511-6)
- [9] A. K. Gangopadhyay, K. F. Kelton, “Effect of rare-earth atomic radius on the devitrification of Al88RE8Ni4 amorphous alloys”, *Philosophical Magazine A*, vol. 80, , pp. 1193-1206, 2000 <https://doi.org/10.1080/01418610008212110>
- [10] N. Bassim, C.S. Kiminami, M. J. Kaufman, M. F. Oliveira, M.N.R.V.Perdigão, W.J. Botta Filho, “Crystallization behavior of amorphous Al84Y9Ni5Co2alloy”, *Materials Science and Engineering A*, 304–306, pp.332-237, 2001 [https://doi.org/10.1016/S0921-5093\(00\)01532-X](https://doi.org/10.1016/S0921-5093(00)01532-X)
- [11] T. Gloriant, D.H. Ping, K. Hono, A. L. Greer, M.D. Baro, “Segregation-controllednanocrystalization in an Al-Ni-La metallic glass”, *Applied Physics Letters*, 92, 103126, 2008, <https://doi.org/10.1063/1.2897303>
- [12] V. Dyakova, G. Stefanov, I. Penkov, D. Kovacheva, N. Marinkov, Y. Mourdjeva, S. Gyurov, “Influence of Zn on Glass Forming Ability and Crystallization Behaviour of Rapidly Solidified Al-Cu-Mg (Zn) alloys”, *Journal of Chemical Technology and Metallurgy*, 57, 6, pp. 622-630, 2020 [https://journal.uctm.edu/node/j2022-3/23\\_21-64\\_br\\_3\\_pp\\_622-630.pdf](https://journal.uctm.edu/node/j2022-3/23_21-64_br_3_pp_622-630.pdf)
- [13] V. L. Dyakova, G. N. Stefanov, D. G. Kovacheva, Y. S. Mourdjeva, N. E. Marinkov, .I. G. Penkov and J. S. Georgiev, Influence of Zr and Zn as minority alloying elements on glass forming ability and crystallization behavior of rapidly solidified AlCuMg ribbons, 2449, *AIP Conference proceedings*, 2022, <https://aip.scitation.org/doi/abs/10.1063/5.0090746>
- [14] V. L. Dyakova, B. R. Tzaneva and Y. G. Kostova, “Influence of Zn as minority alloying element on the uniform and local corrosion of amorphous rapidly solidified AlCuMg(Zn) ribbons”, 2449, *AIP Conference proceedings*, 2022, <https://doi.org/10.1063/5.0090752>
- [15] R. Birringer, H. Gleiter, P. Klein, P. Marquardt, “Nanocrystalline materials an approach to a novel solid structure with gas-like disorder?”, *Physics Letters A*, vol.102, no.8, pp. 365-369, 1984 [https://doi.org/10.1016/0375-9601\(84\)90300-1](https://doi.org/10.1016/0375-9601(84)90300-1)
- [16] M. Gögebakan, M. Okumus, Structure and crystallization kinetics of amorphous Al–Ni–Si alloy, *Materials Science-Poland*, vol. 27, no. 1, 2009, <https://materialsscience.pwr.edu.pl/>
- [17] K.L. Sahoo, R. Sahu, “Glass transition and crystallization of Al–Ni–La based metallic glasses studied by temperature modulated DSC”, *Journal of Non-Crystalline Solids*, 365, , pp. 33-36, 2013 <http://dx.doi.org/10.1016/j.jnoncrsol.2013.01.031>